

# Strengths and limitations of a uniform 3D-LUT approach for digital camera characterization

S. Fischer, P. Myland, M. Szarafanowicz, P. Bodrogi and T.Q. Khanh; Laboratory of Lighting Technology, Technische Universität Darmstadt; 64289 Darmstadt, Germany

## Abstract

Digital color imaging technology has become omnipresent in today's modern life. Digital image capturing and reproduction devices such as smartphones, digital still and video cameras, displays, printers, and color scanners can be found in every home, offering extremely high functionality and flexibility. In order to guarantee qualitatively good results regarding the whole image processing pipeline and to achieve high user acceptance, optimized color conversion and correction algorithms play a crucial role. In this context, a new implementation method of uniform three-dimensional lookup tables (3D-LUTs) based on a standardized pre-measured spectral reflectance database will be presented and applied for the color correction of digital camera systems. The strengths and limitations of such an implementation will be discussed and a performance comparison with the standard  $3 \times 3$  matrix color correction will be conducted. It can be found that the proposed 3D-LUT approach outperforms the matrix method in terms of CIEDE2000 color differences and color reproduction properties, but still has its limitations when it comes to achromatic colors and the representation of color gradients.

## Introduction

In general, the RGB-sensor of a digital camera system does not fulfill the Luther-Ives-condition [1, 2, 3], i.e. the spectral response curves  $r(\lambda)$ ,  $g(\lambda)$ , and  $b(\lambda)$  of the RGB-sensor cannot be described as a linear combination of the eye cone response functions. As a consequence the spectral sensitivity of the camera system differs significantly from the human perception described by the color matching functions  $\bar{x}(\lambda)$ ,  $\bar{y}(\lambda)$ , and  $\bar{z}(\lambda)$  of the CIE 1931 standard observer [4], which can be seen in Fig. 1.

In order to guarantee qualitatively good results, proper camera characterization and color correction are therefore an indispensable part of the image processing pipeline from raw sensor data to the final image displayed on a reproduction device [5, 6]. Especially, when modern LED lighting systems come into play. In Ref. [5], the authors showed that scene-specifically optimized LED emission spectra can lead to improved color reproduction properties of digital camera systems. They further stated that color enhancement with respect to certain color preference metrics was also feasible simply by adjusting the emitted LED spectra accordingly. This holds true as long as the camera system was characterized in such a way that the introduced colorimetric errors are negligibly small.

If the camera system in first approximation provides colorimetrically a one-to-one translation, the long-term goal should therefore be to establish an image enhancement pipeline which is based on the flexibility of LED illumination rather than shifting it to the tedious process of post-production. For this purpose suit-

able camera characterization and color correction algorithms have to be chosen.

Basically, color correction aims at establishing the best possible mapping from device dependent RGB raw data to some device independent color space, typically spanned by the corresponding CIE XYZ values. If a trichromatic camera satisfied the Luther-Ives-condition, its raw RGB responses would be linearly related to the XYZ tristimulus values and a simple  $3 \times 3$  linear transform could be applied without inducing any approximation errors. However, this does not hold true for the vast majority of the digital camera systems available on the market. Hence, in order to account for the systematic non-linearities and to reduce colorimetric errors in the mapping process, various approaches such as polynomial regression [7, 8, 9, 10, 11] and neural networks [12, 13, 14] have been studied in the past leading to quite satisfying results. A third, very promising method which should be discussed in this work is the use of three-dimensional lookup tables (3D-LUTs) for performing the camera characterization and color correction.

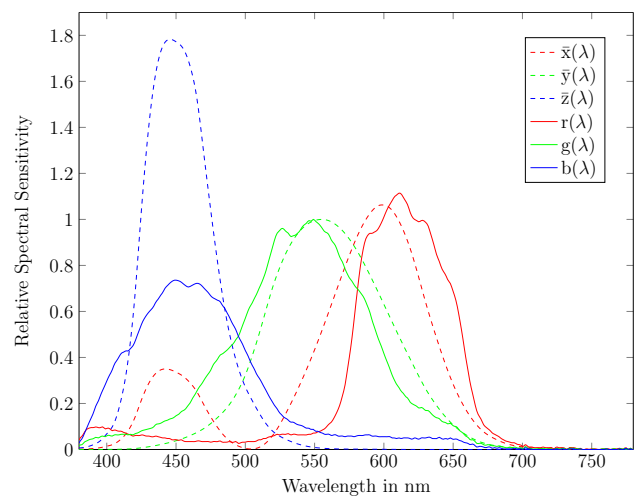


Figure 1. Relative spectral sensitivities of the camera color filters (RGB) compared to the color matching functions  $\bar{x}(\lambda)$ ,  $\bar{y}(\lambda)$ , and  $\bar{z}(\lambda)$  of the CIE 1931 standard observer [4].

Uniform as well as nonuniform 3D-LUTs have extensively been studied in the literature and successfully applied to digital printers and color displays [15, 16, 17, 18, 19, 20]. Basically, a 3D-LUT for color correction directly relates the device dependent signals to some device independent color space using for example empirical methods which in general demand a large number of measurements [21]. As a benefit, highly accurate charac-

terization and color correction can be achieved without knowing the underlying non-trivial functional relationship between the device dependent and the device independent color space. With the prospect of obtaining unprecedented high accuracy, an adequate adaptation of the 3D-LUT approach for digital camera characterization would be most desirable.

The aim of this paper therefore is to present a new implementation method of uniform 3D-LUTs for camera characterization based on a standardized pre-measured spectral reflectance database. Furthermore, the strengths as well as the current limitations of such an implementation will be discussed in terms of CIEDE2000 color differences and visualized color gradients. A comparison with the standard  $3 \times 3$  color correction as defined in Ref. [22] will be performed.

The paper is organized as follows. In Sec. 2 we give a detailed introduction on the creation of a uniform 3D-LUT for digital camera characterization as proposed in this work including the packing, extraction, and interpolation process. Sec. 3 discusses the influence of different parameters on the final interpolation results whereas the color correction and reproduction properties of the 3D-LUT approach are analyzed in Sec. 4. In Sec. 5 we finish the paper with some concluding remarks and an outlook on future developments.

### Three Dimensional Lookup Table for Color Correction

As discussed before, camera color measurement and human perception differ significantly. From Fig. 1 we notice that the red, green, and blue filter curves have little in common with the corresponding color matching functions  $\bar{x}(\lambda)$ ,  $\bar{y}(\lambda)$ , and  $\bar{z}(\lambda)$ , respectively. This mismatching cannot be corrected satisfyingly by using a simple linear transformation and has a major influence on the color reproduction properties of the digital camera system.

In order to improve the color reproduction, we therefore introduce a new camera characterization and color correction method based on a 3D-LUT mapping the device dependent RGB raw data to some device independent color space. Following Ref. [23], building a 3D-LUT for color correction requires three successive phases: (i) packing which describes the partitioning of the RGB camera source space by selecting appropriate sample points from a training set which constitute the lattice points of the LUT, (ii) extraction which aims at finding the location of an arbitrary input RGB value in order to extract the color values of the nearest lattice points, and (iii) interpolation which uses the input values and the extracted lattice points to calculate the color specifications of the input point in destination color space.

Being of fundamental importance for the success and accuracy of the 3D-LUT approach, each of the three phases will thoroughly be discussed in the following.

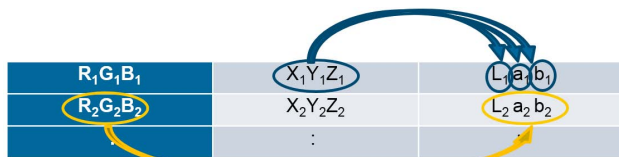


Figure 2. Schematic structure of the training data used for creating the uniform 3D-LUT mapping raw camera data to device independent color space.

### Partitioning of the RGB source space

For the partitioning of the RGB camera source space a training set is needed. Here, the standard object color spectra (SOCS) database has been chosen. This database standardized in ISO/TR 16066:2003 [24] was developed for the evaluation of the color-sensor quality of image capturing devices [25, 26] and contains more than fifty thousand reflectance spectra of real-measured objects.

For each database entry the corresponding XYZ tristimulus values, CIELAB coordinates and raw RGB sensor data are calculated assuming reference illuminant D65. As a result, we obtain more than fifty thousand coordinate pairs of  $RGB \rightarrow XYZ/L^*a^*b^*$  as illustrated in Fig. 2, which form as a training set the basis for creating a uniform 3D-LUT mapping digital camera raw data to the device independent CIELAB color space.

In general, a uniform 3D-LUT consists of an equidistant sampling of dimension  $d$  along each axis of the RGB camera source space as illustrated in Fig. 3. This leads to a total number of  $d^3$  lattice points defining  $(d-1)^3$  interpolation cubes. Thus, for each given lattice point in RGB source space the corresponding values in  $L^*a^*b^*$  destination space have to be calculated from the training set first and tabulated into the LUT. The destination space values of nonlattice points lying within a certain cube can then be interpolated by using both the RGB and  $L^*a^*b^*$  coordinates of the nearest lattice points. Further details on the interpolation process will be discussed later.

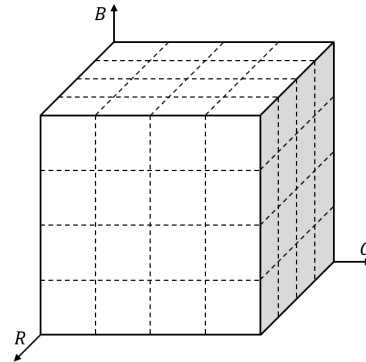


Figure 3. Illustration of a five dimensional 3D packing [23].

In order to select appropriate sample points which constitute the equidistantly spaced lattice points of the uniform 3D-LUT, a local linear regression approach is applied to the training data. For each lattice point  $RGB_i$ , the six nearest (Euclidean) RGB values from the training set and their corresponding XYZ values are chosen to calculate a  $3 \times 3$  local matrix  $A_i$  which performs the mapping from RGB to XYZ in this part of the training set.

The optimal  $A_i$  can be obtained by a distance-weighted least-squares regression which minimizes the mean squared error metric of the linear fit to the six training samples. Mathematically, this can be written as

$$\begin{aligned} & \underset{A_i}{\text{minimize}} \quad \left( \frac{1}{6} \sum_{n=1}^6 \|XYZ_n - A_i \cdot RGB_n\|^2 \cdot w(d_n) \right), \\ & \text{subject to} \quad A_i \cdot (255, 255, 255)^T = (95.047, 100, 108.883)^T, \\ & \quad \quad \quad A_i \cdot RGB_i \geq (0, 0, 0)^T, \end{aligned}$$

where  $\|\cdot\|$  denotes the Euclidean norm giving the length of the error vector and the weighting factor  $w(d_n) = (d_n^\rho + \epsilon)^{-1}$  inversely depends on the Euclidean distance  $d_n$  between the lattice point  $RGB_i$  and the  $n$ th selected training sample  $RGB_n$  for calculating the local matrix  $A_i$ . It is chosen in such a way that training points that are distant from the lattice point are less weighted in the error metric and, therefore, in the data fitting process than nearby samples. The smoothness and locality of the data fitting can directly be controlled by the two parameters  $\rho$  and  $\epsilon$  [21, 30].

The matrices  $A_i$  are finally used to estimate the tristimulus values  $XYZ_i$  of each lattice point  $RGB_i$ . In this context, the two additional constraints on the matrices  $A_i$  guarantee white point preservation to D65 and avoid the invalid mapping to negative  $XYZ$  values. The resulting  $XYZ_i$  values are then transformed to  $L^*a^*b^*$  coordinates, leading to the final form of our 3D-LUT that can eventually be used to calculate device independent  $L^*a^*b^*$  from arbitrary raw  $RGB$  input data.

### Extraction and Interpolation Process

After the creation of the uniform 3D-LUT from a set of training data described in the previous section, an extraction and interpolation algorithm has to be implemented in the next step.

Given an arbitrary  $RGB$  input value, the extraction algorithm locates the dedicated cube and, therefore, finds the lattice points required for the computation of the corresponding  $L^*a^*b^*$  destination space coordinates. Due to the equally spaced packing of the uniform 3D-LUT, an efficient extraction algorithm can easily be implemented following Refs. [23, 31]: If in 8bit quantization each  $RGB$  axis is divided into  $(d - 1) = 2^j$  equal sections where  $j < 8$  is an integer, the nearest lattice points can be directly obtained from the most significant  $j$  bits of the  $RGB$  input along each axis. Being based on masking and shifting bits, this procedure is computationally much faster than performing comparison operations and allows for an efficient determination of the proper interpolation borders.

For the subsequent interpolation various methods are reported in the literature [21, 23, 31]. However, due to its computational simplicity but also promising accuracy, a tetrahedral interpolation technique has been chosen. As can be seen from Fig. 4, tetrahedral interpolation subdivides a cube which is spanned by eight lattice points into six different tetrahedra sharing one common edge representing the diagonal of the cube along the neutral axis in  $RGB$  space leading to improved accuracy in the reproduction of color gradients.

Within a tetrahedron the interpolation can be performed using the four associated lattice points. Given an arbitrary  $RGB$  input value, an average of 2.5 comparison tests for determining the corresponding tetrahedron and three linear interpolations [21] are necessary to calculate the corresponding  $L^*a^*b^*$  coordinates given by

$$L^*a^*b^* = c_0 + c_1 \frac{\Delta R}{k} + c_2 \frac{\Delta G}{k} + c_3 \frac{\Delta B}{k}, \quad (1)$$

where  $\Delta R = R - R_{000}$ ,  $\Delta G = G - G_{000}$ , and  $\Delta B = B - B_{000}$ . Here,  $R_{000}$ ,  $G_{000}$ , and  $B_{000}$  are the coordinates in  $RGB$  space of the lower left point as indicated in Fig. 4 and  $k$  is the edge length of the interpolation cubes defining the step size of the uniform 3D-LUT as shown in Fig. 3. The interpolation coefficients  $c_0$ ,  $c_1$ ,  $c_2$ , and  $c_3$  can be calculated from the  $L^*a^*b^*$  coordinates of the lattice

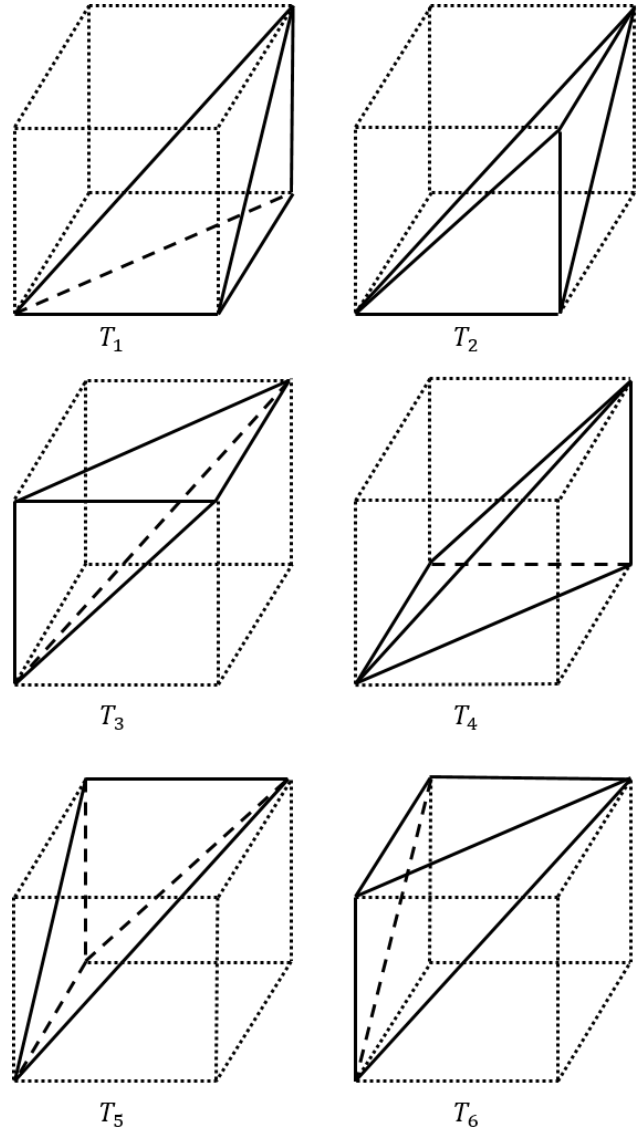


**Figure 4.** Overview of the tetrahedral interpolation scheme. The interpolation cube spanned by eight lattice points is divided into six different tetrahedra sharing the cube diagonal. Within each tetrahedron the interpolation of an arbitrary  $RGB$  input value can be performed using the four associated lattice points [31].

points and depend on the tetrahedron used for interpolation. An overview is given in Table 1.

Hence, tetrahedral interpolation offers an efficient and accurate method for calculating device independent  $L^*a^*b^*$  coordinates from raw  $RGB$  camera input data while greatly reducing the computational costs compared to other linear interpolation techniques.

### Influence of Interpolation Parameters

Throughout the whole packing, extraction, and interpolation process introduced in the previous sections three different, essential parameters influencing the quality and accuracy of the final interpolation results can be identified. These parameters are the

**Table 1 – Applied inequality relations and corresponding coefficients  $c_0, c_1, c_2,$  and  $c_3$  as implemented for tetrahedral interpolation. Note that each possible tetrahedron gives its own inequality relation leading to different interpolation coefficients.**

Tetrahedron	Condition	$c_0$	$c_1$	$c_2$	$c_3$
$T_1$	$\Delta R > \Delta G > \Delta B$	$L^*a^*b_{000}^*$	$L^*a^*b_{100}^* - L^*a^*b_{000}^*$	$L^*a^*b_{110}^* - L^*a^*b_{100}^*$	$L^*a^*b_{111}^* - L^*a^*b_{110}^*$
$T_2$	$\Delta R > \Delta B > \Delta G$	$L^*a^*b_{000}^*$	$L^*a^*b_{100}^* - L^*a^*b_{000}^*$	$L^*a^*b_{111}^* - L^*a^*b_{101}^*$	$L^*a^*b_{101}^* - L^*a^*b_{100}^*$
$T_3$	$\Delta B > \Delta R > \Delta G$	$L^*a^*b_{000}^*$	$L^*a^*b_{101}^* - L^*a^*b_{001}^*$	$L^*a^*b_{111}^* - L^*a^*b_{101}^*$	$L^*a^*b_{001}^* - L^*a^*b_{000}^*$
$T_4$	$\Delta G > \Delta R > \Delta B$	$L^*a^*b_{000}^*$	$L^*a^*b_{110}^* - L^*a^*b_{010}^*$	$L^*a^*b_{010}^* - L^*a^*b_{000}^*$	$L^*a^*b_{111}^* - L^*a^*b_{110}^*$
$T_5$	$\Delta G > \Delta B > \Delta R$	$L^*a^*b_{000}^*$	$L^*a^*b_{111}^* - L^*a^*b_{011}^*$	$L^*a^*b_{010}^* - L^*a^*b_{000}^*$	$L^*a^*b_{011}^* - L^*a^*b_{010}^*$
$T_6$	$\Delta B > \Delta G > \Delta R$	$L^*a^*b_{000}^*$	$L^*a^*b_{111}^* - L^*a^*b_{011}^*$	$L^*a^*b_{011}^* - L^*a^*b_{001}^*$	$L^*a^*b_{001}^* - L^*a^*b_{000}^*$

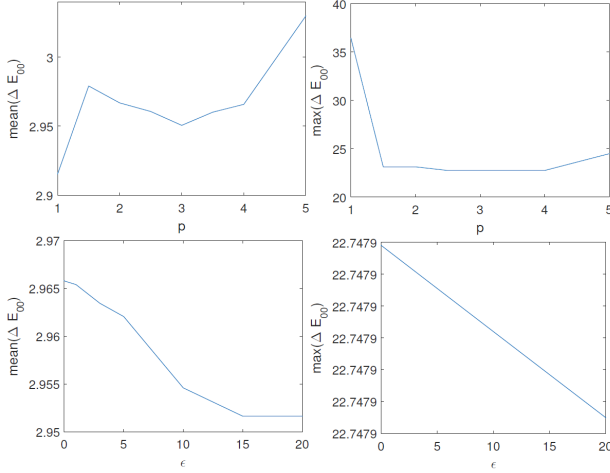


**Figure 5.** Mean (left) and maximum (right) CIEDE2000 color differences of the Leeds-1000 test set as a function of the weighting parameters  $\rho$  (upper row) and  $\epsilon$  (lower row). The dependence of the final interpolation results on the two parameters  $\rho$  and  $\epsilon$  is observed to be quite weak.

weighting parameters  $\rho$  and  $\epsilon$  of the weighting factor  $w(d_n)$  as well as the step size parameter  $k$  giving the edge length of the interpolation cubes. The influence of these parameters on the final interpolation results will be discussed in the following.

In order to obtain a quality measure, the Leeds-1000 spectral database [32] has been chosen as a test set being not included in the training set. This database contains one thousand representative reflectance spectra derived from approximately one hundred thousand real measured objects. First, we calculate the corresponding CIELAB values denoted by  $L^*a^*b_{i,calc}^*$  under reference illuminant D65 as well as their representations  $RGB_{i,calc}$  in camera source space, where  $i = 1, 2, \dots, 1000$ .

Next, the uniform 3D-LUT is built from the SOCS training data as described above using different parameters  $\rho$ ,  $\epsilon$ , and  $k$ . For each set of parameters, the resulting LUT is then used to estimate device independent CIELAB coordinates  $L^*a^*b_{i,est}^*$  from the  $RGB_{i,calc}$  input data. Finally, the CIEDE2000 formula [33] is used for evaluating the perceivable color differences  $\Delta E_{00,i}$  between the directly calculated and the estimated CIELAB coordinates. Thus, the mean and the maximum of the CIEDE2000 color differences of all Leeds-1000 test colors can be considered as a measure for the quality and accuracy of our 3D-LUT approach. The smaller both quantities are the better the mapping between  $RGB$  input signals and device independent  $L^*a^*b^*$  coordinates is

performed leading to good color reproduction properties of the digital camera system.

### Weighting Parameters

As mentioned earlier in this paper, the weighting function  $w(d_n)$  depends on the two weighting parameters  $\rho$  and  $\epsilon$  giving a direct control on the smoothness and the locality of the data fitting process. For increasing  $\rho$ , the weighting function  $w(d_n)$  supports a more local behavior since the influence of the training samples for calculating the local matrices  $A_i$  decreases more rapidly as a function of the distance from the corresponding lattice points. On the other hand, a large value of  $\epsilon$  results in a more global regression as the weighting function  $w(d_n)$  becomes less sensitive to the distance [21, 30]. Hence, finding the optimal parameters  $\rho$  and  $\epsilon$  is always a trade-off between overall smoothness and local accuracy.

In this study, the optimal parameters for the specifically chosen training and test set were found by a heuristic trial and error approach trying to minimize both the mean and the maximum CIEDE2000 color differences of the test colors using a step size of  $k = 16$  for building the 3D-LUT.

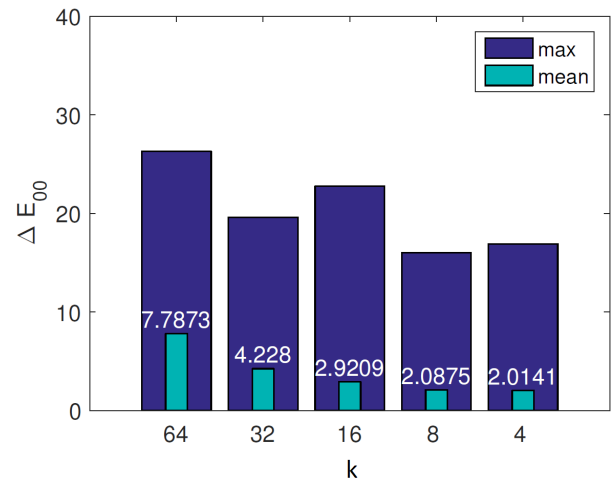


**Figure 6.** Mean and maximum CIEDE2000 color differences of the Leeds-1000 test colors as a function of the step size parameter  $k$ . With decreasing  $k$  the color differences can be reduced. The higher the resolution of the 3D-LUT the better the quality and accuracy of the color correction.

It should be noted that the dependence of the the final interpolation results on the two parameters  $\rho$  and  $\epsilon$ , as illustrated in Fig. 5 in terms of the mean and the maximum CIEDE2000 color



on the right obtained via the 3D-LUT approach is almost indistinguishable from the reference on the left, whereas the matrix method in the middle consistently produces too much lightness. This again indicates the better overall color reproduction properties of the 3D-LUT approach. However, perceivable deviations can also be observed for the LUT when applied to the achromatic patches revealing the limitations of the current approach. Thus, for future developments a solution has to be found to enhance the reproduction properties of the current 3D-LUT approach for achromatic colors.

### Color Gradients

Another big challenge for any color correction method is the proper reproduction of well-defined color gradients. In Fig. 9 several different color gradients given as three dimensional lines in *RGB* camera source space (see Fig. 10) have been calculated and visualized. This allows for a direct comparison of the performance of the matrix method (lower bar of each color gradient) with the results obtained by using the 3D-LUT approach (upper bar of each color gradient).

Basically, the matrix method gives slightly smoother color gradients due to its global character, which is especially obvious at the beginning and at the end of the color gradients where the corresponding *RGB* values are far outside the gamut of the SOCS training set used for building the 3D-LUT which finally performs the mapping. Furthermore, the color gradients (2) and (4) that pass the achromatic axis show distinct jumps and a non-smooth behavior for the achromatic colors. Being in accordance with the conclusions of the previous section, additional research is therefore necessary to improve the performance of the uniform 3D-LUT when applied to achromatic or near-achromatic colors.

### Conclusion and Outlook

In this paper we proposed a new implementation method of uniform 3D-LUTs for camera characterization based on a standardized pre-measured spectral reflectance database which has been used as a training set for building the 3D-LUT. In order to obtain a uniformly-spaced three dimensional packing, a distance-weighted local linear regression algorithm has been implemented for estimating the  $L^*a^*b_i^*$  coordinates of the equidistant lattice points *RGB<sub>i</sub>* from the training data. Arbitrary *RGB* input data can eventually be mapped to device independent CIELAB color space by using a fast and efficient tetrahedral interpolation technique.

Different parameters influencing the final interpolation results have been tested and analyzed in terms of CIEDE2000 color differences. It was found that the step size *k* is the most significant parameter for the specifically chosen training and test set used in this work. The smaller the step size the larger the resolution of the 3D-LUT leading to a better performance regarding the quality and accuracy of the color correction.

Finally, we analyzed the color correction and reproduction properties of the proposed 3D-LUT approach and compared its performance with the ISO standardized procedure for camera characterization using a non-linearly optimized  $3 \times 3$  matrix. We found that our 3D-LUT approach outperforms the matrix method and offers better color reproduction properties for most of the test colors. However, the approach has its limitations when it comes to achromatic colors and the representation of color gradients.

In contrast to the matrix method which gives pretty smooth

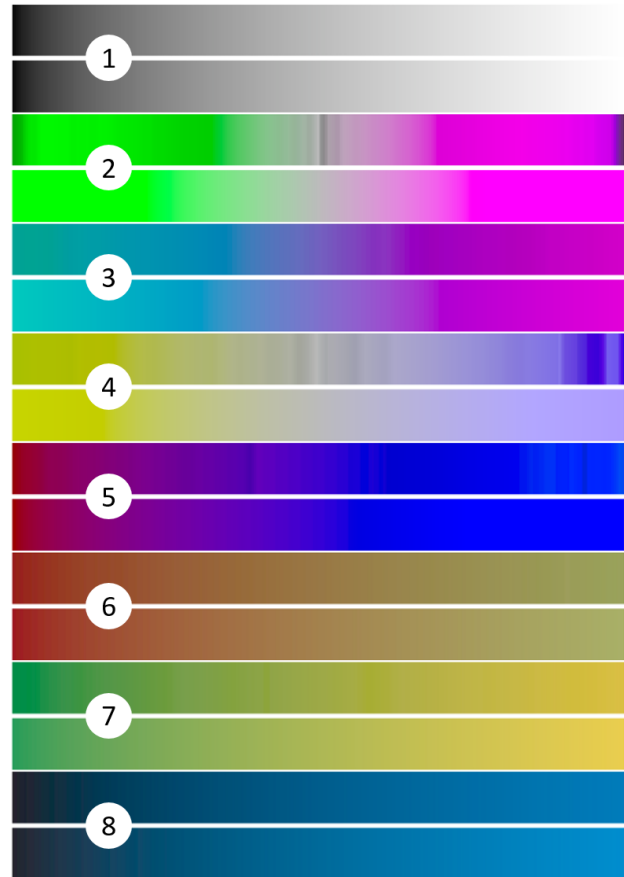


**Figure 9.** Reproduction of various color gradients as defined in Fig. 10. The results obtained by using the 3D-LUT approach (upper bar) are compared to the performance of the matrix method (lower bar). The matrix method gives smoother gradients due to its more global character. Especially at the beginning and at the end of the color gradients the deficiencies of the 3D-LUT approach become apparent. Numbers 1-8 assign each visualized color gradient to its corresponding representation in *RGB* source space as shown in Fig. 10.

color gradients due to its global character, the 3D-LUT approach shows distinct jumps and non-smooth behavior, especially at the beginning and the end of the gradients where the corresponding *RGB* values are far outside the gamut of the training set, which can be seen in Fig. 10. Here, training data that are far distant from the actual lattice points have to be used for calculating the corresponding  $L^*a^*b^*$  coordinates leading to relatively large errors and, eventually, to a false representation in the color gradients. A possible improvement could be achieved by adding additional data to the training set filling the void in the *RGB* source space. This might also improve the reproduction of achromatic colors. If one for example includes the Leeds-1000 test set in the training data the mean and the maximum color differences can be both reduced by 30% and somewhat smoother color gradients can be observed.

However, special care must be taken since a simple enclosing of additional spectra from arbitrary databases might also increase the redundancy of some *RGB* values in the training data causing metameric effects. This means that one single *RGB* training point

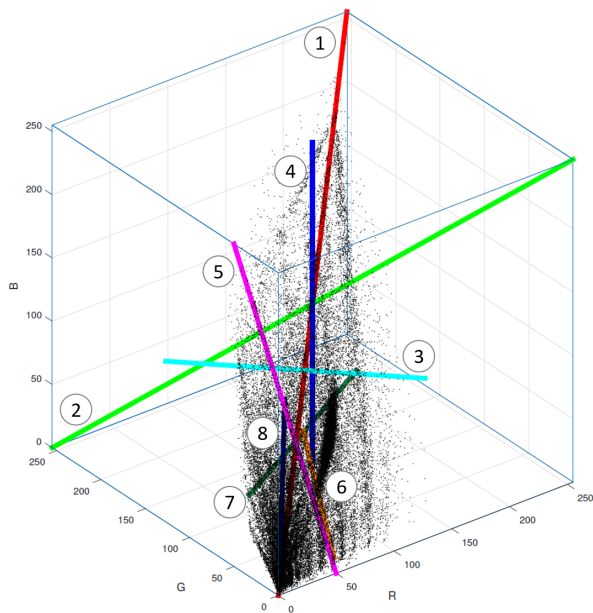


**Figure 10.** Three dimensional lines in RGB camera source defining the color gradients visualized in Fig. 9. Numbers 1-8 indicate their relation. Note that the start and end points of some of the gradient lines lie far outside the Gamut of the SOCS training set indicated by the black points resulting in the poor performance of the 3D-LUT in this part of the RGB space.

could have multiple  $XYZ/L^*a^*b^*$  output data. Since the current implementation of the packing algorithm simply searches for the six closest  $RGB \rightarrow XYZ$  pairs to the lattice points whose  $L^*a^*b^*$  coordinates should be determined, it may happen that six training points with exactly the same  $RGB$  but slightly different  $XYZ$  are chosen from the training set. This will most probably lead to a local matrix which is unsuitable for a proper reproduction of the corresponding lattice point resulting in large interpolation errors. Hence, we must either increase the number of training points used for the local linear regression or an intelligent and more complex sampling method for selecting appropriate training data must be implemented. First tests showed that increasing the number of training points from six to fifty gives much smoother color gradients comparable to those obtained via the matrix method while keeping the mean and the maximum color differences more or less the same. Unfortunately, this drastically increases the computational time required to perform the local linear regression at each lattice point and, therefore, a trade-off has to be found.

Finally, it should be noted that this work created the basis for further research on all aspects of the 3D-LUT approach for digital camera characterization. Probably, a combination of all improvement proposals discussed in this section will eventually lead to a characterization method that outperforms all other approaches regarding its color correction and reproduction properties. In particular, the smoothness problem needs to be fixed in order to make our approach applicable for real imaging applications. A Gaussian weighting of the training data with a standard deviation larger than the grid point distance might solve or at least improve this issue. Besides, it is also thinkable to expand our approach to nonuniform 3D-LUTs which offer more flexibility by tweaking the lattice points in such a way that color differences are

further reduced and color gradients may appear smoother. Ongoing research on these topics is currently being performed by our group.

## Funding

This work is part of the Project UNILED-II ("Development of Quality Criteria, Evaluation Methods and Standards for Smart LED-Lighting Solutions") funded by the German Federal Ministry of Education and Research (BMBF).

## References

- [1] R. Luther, "Aus dem Gebiet der Farbreizmetrik," *Z. Tech. Phys.* **8**, 540 (1927).
- [2] N. Ohta and A.R. Robertson, "Measurement and Calculation of Colorimetric Values, in *Colorimetry: Fundamentals and Applications*," John Wiley & Sons Ltd (2005).
- [3] F. Martínez-Verdú et al., "Concerning the calculation of the color gamut in a digital camera," *Color Res. Appl.* **31**, 399 (2006).
- [4] CIE Publication 015:2004, "Colorimetry," 3rd Edition, Commission Internationale de l'Eclairage (2004).
- [5] S. Fischer and T. Q. Khanh, "Color Reproduction of Digital Camera Systems Using LED Spotlight Illumination," *Proceedings of the 23rd Color and Imaging Conference*, 143 (2015).
- [6] V. Cheung et al., "A comparative study of the characterisation of colour cameras by means of neural networks and polynomial transforms," *Color. Technol.* **120**, 19 (2004).
- [7] M. J. Vrhel, "Mathematical methods of color correction," PhD thesis, North Carolina State University, Department of Electrical and Computer Engineering (1993).
- [8] T. Johnson, "Methods for characterizing color scanners and digital cameras", *Displays* **16**(4), 83 (1996).
- [9] G. D. Finlayson and M. S. Drew, "Constrained least-squares regression in color spaces," *J. Electron. Imag.* **6**, 484 (1997).
- [10] P. G. Herzog et al., "Colorimetric characterization of novel multiple-channel sensors for imaging and metrology," *J. Electron. Imaging* **8**(4), 342 (1999).
- [11] G. Hong, M. R. Luo, and P. A. Rhodes, "A Study of Digital Camera Colorimetric Characterization Based on Polynomial Modeling," *Color Res. Appl.* **26**, 76 (2001).
- [12] H. R. Kang and P. G. Anderson, "Neural network applications to the color scanner and printer calibrations," *J. Electron. Imaging* **1**(2), 125 (1992).
- [13] T. L. V. Cheung and S. Westland, "Color camera characterisation using artificial neural networks," *Proceedings of the 10th Color and Imaging Conference*, 117 (2002).
- [14] L. Xinwu, "A new color correction model for digital cameras based on BP neural network," *Adv. Inf. Sci. Service Sci* **3**(5), 72 (2011).
- [15] P.-C. Hung, "Colorimetric calibration in electronic imaging devices using a look-up table method and interpolations," *J. Electron. Imaging* **2**(1), 53 (1993).
- [16] J. M. Kasson, W. Plouffe, S. I. Nin, "A tetrahedral interpolation technique for color space conversion," *Proceedings of the SPIE* **1909**, 127 (1993).
- [17] H. R. Kang, "Comparisons of three-dimensional interpolation techniques by simulations," *Proceedings of the SPIE* **2414**, 104 (1995).
- [18] V. Monga, R. Bala, "Sort-select-damp: An efficient strategy for color look-up table lattice design," *Proceedings of the 16th Color and Imaging Conference*, 247 (2008).
- [19] E. Garcia, M. Gupta, "Building Accurate and Smooth ICC Profiles

- by Lattice Regression,” Proceedings of the 17th Color and Imaging Conference, 101 (2009).
- [20] V. Monga, R. Bala, “Algorithms for color look-up-table (LUT) design via joint optimization of node locations and output values,” IEEE International Conference on Acoustics Speech and Signal Processing (ICASSP), 998 (2010).
- [21] G. Sharma, “Digital Color Imaging Handbook,” CRC Press, Inc., Boca Raton, FL, USA (2002).
- [22] ISO 17321-1:2012, “Graphic technology and photography – Colour characterization of digital still cameras (DSCs), Part 1: Stimuli, metrology and test procedures,” International Organization for Standardization (2012).
- [23] H. R. Kang, “Computational Color Technology,” The International Society for Optical Engineering (2006).
- [24] ISO/TR 16066:2003, “Graphic technology – Standard object colour spectra database for colour reproduction evaluation (SOCS),” International Organization for Standardization (2003).
- [25] J. Tajima et al., “Development and standardization of a spectral characteristics database for evaluating color reproduction in image input devices,” Proceedings of the SPIE **3409**, 42 (1998).
- [26] J. Tajima, M. Inui, and Y. Azuma, “Development of standard object colour spectra database for colour reproduction evaluation (SOCS),” J. Soc. Photogr. Sci. Technol. Japan **62**, 126 (1999).
- [27] G. Wyszecki and W. S. Stiles, “Color Science: Concepts and Methods, Quantitative Data and Formulae,” 2nd Edition, Wiley Classics Library (2000).
- [28] M. D. Fairchild, “Color Appearance Models,” 2nd Edition, John Wiley & Sons Ltd (2005).
- [29] R. W. G. Hunt and M. R. Pointer, “Measuring Colour,” 4th Edition, John Wiley & Sons Ltd (2011).
- [30] R. Balasubramanian, M. S. Maltz, “Refinement of printer transformations using weighted regression,” Proceedings of the SPIE **2658**, 334 (1996).
- [31] H. R. Kang, “Color Technology for Electronic Imaging Devices,” The International Society for Optical Engineering (1997).
- [32] K. Smet, J. Schanda, L. Whitehead, and R. Luo, “CRI2012. A proposal for updating the CIE colour rendering index,” Lighting Res. Technol. **45**, 689 (2013).
- [33] M. R. Luo, G. Cui, B. Rigg, “The development of the CIE 2000

colour-difference formula: CIEDE2000,” Color Res. Appl. **26**(5), 340 (2001).

## Author Biography

Sebastian Fischer received his M.Sc. in Physics from the Technische Universität Darmstadt, Germany (2014). Since then he has been working at the Laboratory of Lighting Technology in Darmstadt as a research assistant and PhD student. His current work is focused on digital cine technique and camera technology.

Paul Myland is a graduate student at the Laboratory of Lighting Technology at the Technische Universität Darmstadt, Germany. He received his B.Sc. in Electrical Engineering from the Technische Universität Darmstadt, Germany in 2014. In his work, he was concerned with the application of a 3D-LUT approach for digital camera characterization. At the moment, he is gathering industrial experience as an intern at ARRI Cine Technik in Munich, Germany.

Matthias Szarafanowicz received his M.Sc. in Quantum Optics from the Technische Universität Darmstadt in 2014. The same year, he started working at the Laboratory of Lighting Technology in Darmstadt as a research assistant and PhD student. His research interests include color sensing technologies, smart LED lighting systems, and human color perception.

Peter Bodrogi is Senior Researcher at the Laboratory of Lighting Technology at the Technische Universität Darmstadt, Germany. In 1993, he graduated in Physics from the Lorand Eötvös University (Budapest). In 1999, he obtained his PhD degree in Information Technology from the University of Pannonia and in 2010 his Degree of Lecture Qualification from the Technische Universität Darmstadt. His research interests include: lighting engineering, color science, colorimetry, LEDs, optimization of self-luminous displays, mesopic visual performance.

Tran Quoc Khanh is University Professor and Head of the Laboratory of Lighting Technology at the Technische Universität Darmstadt, Germany. He graduated in Optical Technologies and obtained his PhD in Lighting Engineering from the Technische Universität Ilmenau, Germany. Before being appointed as a professor, he gathered industrial experience as a project manager at ARRI Cine Technik in Munich, Germany. His research interests cover all important aspects of modern lighting technology including LEDs, colorimetry, mesopic vision, glare, photometry and color science related topics.